Regulatory Effects of the Wnt7b/β-Catenin/MMP-2 Signaling Pathway on Scleral Stiffness in Guinea Pigs With Form-Deprivation Myopia

Binyu Wen,[1] Hangyu Li,[2,3] Hui Tao,[1] Hong Ren,[1] Bosheng Ma,[1] Mengdi Shi,[1] Shen Chen,[1] Jiaqi Du,[1] Ziyi Cai,[1] Jing Zhang,[1] Dongshi Guan,[2,3] and Zhihong Deng[1]

[1]Department of Ophthalmology, The Third Xiangya Hospital, Central South University, Changsha, Hunan, China
[2]State Key Laboratory of Nonlinear Mechanics, Institute of Mechanics, Chinese Academy of Sciences, Beijing, China
[3]School of Engineering Science, University of Chinese Academy of Sciences, Beijing, China

Correspondence: Dongshi Guan, State Key Laboratory of Nonlinear Mechanics, Institute of Mechanics, Chinese Academy of Sciences, No. 15, Bei Si Huan Xi Road, Beijing 100191, China; dsguan@imech.ac.cn.
Zhihong Deng, Department of Ophthalmology, The Third Xiangya Hospital, Central South University, 138 Tongzipo Rd., Yuelu District, Changsha, Hunan 410013, China; 602073@csu.edu.cn.

BW and HL contributed equally to the work presented here and should therefore be regarded as equivalent authors.

Received: July 2, 2024
Accepted: April 12, 2025
Published: May 8, 2025

Citation: Wen B, Li H, Tao H, et al. Regulatory effects of the Wnt7b/β-Catenin/MMP-2 signaling pathway on scleral stiffness in guinea pigs with form-deprivation myopia. *Invest Ophthalmol Vis Sci.* 2025;66(5):19. https://doi.org/10.1167/iovs.66.5.19

Purpose. The development and progression of myopia are influenced by the Wnt7b/β-catenin signaling pathway. This study investigated the specific impacts of this pathway on the biomechanical properties of the sclera by altering the expression of matrix metalloproteinase-2 (MMP-2) to regulate type I collagen (collagen I) levels.

Methods. We examined the effects of the Wnt7b/β-catenin signaling pathway and MMP-2 on human fetal scleral fibroblasts (HFSFs) and the sclera of guinea pigs with form-deprivation myopia (FDM). To explore the effects of the Wnt7b/β-catenin pathway and the role of MMP-2 in this context, we treated HFSFs and guinea pig sclera with specific agonists and inhibitors targeting Wnt7b/β-catenin and MMP-2. The expression levels of Wnt7b, MMP-2, and collagen I were subsequently analyzed quantitatively via western blot (WB) analysis, immunofluorescence, and quantitative real-time PCR (qRT-PCR) to assess protein and mRNA changes in response to pathway manipulation. Atomic force microscopy (AFM) was used to measure the elastic modulus of the treated HFSFs and guinea pig sclera to directly evaluate changes in cell and tissue stiffness. In the FDM model, essential ocular parameters such as refractive error and axial length (AL) were also assessed.

Results. In vivo and in vitro activation of the Wnt7b/β-catenin signaling pathway significantly upregulated MMP-2 expression, which was accompanied by a notable decrease in collagen I levels. This change led to a reduction in the elastic modulus of both HFSFs and the sclera of guinea pigs with FDM. These significant biomechanical changes in the scleral tissue were indicated by a reduction in stiffness. Alterations in scleral biomechanics were associated with changes in ocular parameters, including an increase in AL and a myopic shift in refraction.

Conclusions. The Wnt7b/β-catenin pathway regulates scleral biomechanics by upregulating MMP-2 expression, which leads to increased collagen I degradation and, consequently, an increase in axial elongation and a myopic shift in refractive error.

Keywords: Wnt7b/β-catenin, MMP-2, collagen I, scleral stiffness, form-deprivation myopia

Myopia is characterized by the inability of parallel light rays to focus on the retina, resulting in unclear images, typically due to excessive axial eye length elongation.[1] Epidemiological studies indicate that the prevalence of myopia in adults ranges from 10% to 30% globally, with some areas in East Asia and Southeast Asia experiencing rates as high as 80% to 90% among young people.[2,3] Severe pathological myopia can lead to serious complications that cause substantial and irreversible vision loss, including retinal detachment, choroidal neovascularization, and macular degeneration blindness.[4–7]

The most notable anatomical changes during myopia progression are abnormal increases in axial length (AL) and substantial thinning of the sclera.[8,9] Scleral thinning primarily results from the abnormal degradation of the extracellular matrix (ECM).[10] Type I collagen (collagen I) is the major component of the scleral ECM.[9] Previous studies have shown that the upregulation of matrix metalloproteinase-2 (MMP-2) expression is linked to the development of myopia.[11–13] Moreover, MMP-2 is a crucial enzyme involved in degradation of the ECM.[14,15] In mice with form-deprivation myopia (FDM), scleral hypoxia leads to an increase in hypoxia-inducible factor 2α (HIF-2α) expression, which in turn promotes myopia progression by increasing the expression of MMP-2 and accelerating the degradation of collagen I.[16]

The Wnt7b/β-catenin signaling pathway has been confirmed to regulate AL elongation to promote the development of myopia.[17] Previous studies have revealed that the expression of essential proteins of the Wnt/β-catenin

signaling pathway, including Wntless (WLS), β-catenin, and T-cell factor 4 (TCF4), is significantly increased in the sclera of mice with FDM, preceding alterations in refraction and AL.[18] Furthermore, genome-wide association studies on human myopia have demonstrated that Wnt family member 7B (WNT7B) is significantly associated with AL and high myopia.[19] However, the precise interplay between the Wnt7b/β-catenin signaling pathway and MMP-2 or collagen I remains poorly understood.

The biomechanical properties of the sclera, such as the elastic modulus and stiffness, are pivotal to the development of myopia.[9] The elastic modulus (stiffness) refers to how much stress (force) is required to generate reversible deformation.[20–22] These properties are influenced primarily by the collagen-rich ECM, which maintains the structural integrity of the sclera. Scleral fibroblasts, which are responsible for synthesizing ECM components, play crucial roles in modulating these biomechanical properties. These cells respond to retinal signaling cascades, remodeling the sclera and altering the ECM composition and scleral collagen organization.[23–25] Thus, examining changes in the biomechanical properties of scleral fibroblasts and scleral tissue during myopia progression is crucial for gaining a complete understanding of myopia development.

In this study, we investigated the role of the Wnt7b/β-catenin signaling pathway and MMP-2 in regulating scleral biomechanics and their potential contributions to myopia progression. We hypothesized that activation of the Wnt7b/β-catenin signaling pathway results in increased MMP-2 expression, which in turn promotes the degradation of collagen I. This process is anticipated to reduce scleral stiffness, thereby contributing to axial elongation and ultimately driving the progression of myopia. To test this hypothesis, we manipulated the activities of both MMP-2 and the Wnt7b/β-catenin pathway in human fetal scleral fibroblasts (HFSFs) and evaluated their effects on collagen I degradation and the elastic modulus of HFSFs. Furthermore, we manipulated the activity of the Wnt7b/β-catenin pathway and MMP-2 expression in the sclera of guinea pigs with FDM during myopia development and investigated the effects of these manipulations on scleral collagen I levels and scleral stiffness.

Methods

Cell Culture

HFSFs (1101HUM-PUMC000139) were obtained from the Cell Resource Center at the Institute of Basic Medical Sciences, Chinese Academy of Medical Sciences. The cells were cultured in high-glucose Dulbecco's Modified Eagle Medium (DMEM, 11995065; Thermo Fisher Scientific, Waltham, MA, USA) supplemented with 1% penicillin–streptomycin (BL505A; Biosharp, Hefei City, China) and 10% fetal bovine serum (FBS, 10099158; Thermo Fisher Scientific). Cultures were maintained at 37°C in a humidified incubator with 5% CO_2. When the cells reached 70% confluence, they were treated for 24 hours with specific agonists or inhibitors. SKL2001 (SKL, HY-101085, 71.38 µM; MedChemExpress, Monmouth Junction, NJ, USA) and teplinovivint (TEP, HY-137454, 60 µM; MedChemExpress) were used to manipulate the Wnt7b/β-catenin signaling pathway as an agonist and inhibitor, respectively, whereas oxidized glutathione (Glu, HY-D0844, 2.48 mg/mL; MedChemExpress) and ARP-100 (ARP, HY-103444, 13.86 nM; MedChemExpress) were used as agonists and inhibitors of MMP-2, respectively. After 24 hours of treatment, Wnt7b, MMP-2, and collagen I expression levels were analyzed using western blotting (WB), immunofluorescence (IF) staining, and quantitative real-time PCR (qRT-PCR).

IF Staining

HFSFs were cultured in 24-well plates (702002; NEST Biotechnology, Jiangsu, China) containing poly-L-lysine-coated glass slides. When the cells reached 70% confluence, they were subjected to 24 hours of pharmacological treatment. Anti–MMP-2 (ab92536; Abcam, Cambridge, UK) or anti-collagen I (ab138492; Abcam) antibodies were incubated with the cells on the slides overnight at 4°C. The following day, the cells were washed with phosphate-buffered saline (PBS) and then incubated with secondary antibodies (ab138492, ab150077, and ab150079; Abcam) for 1 hour at room temperature in the dark. After another PBS wash, the cells were stained with 4′,6-diamidino-2-phenylindole (DAPI, S2110; Solarbio, Beijing, China) in the dark for 10 minutes to visualize the cell nuclei. An N2-DMi8 inverted fluorescence microscope (Leica, Wetzlar, Germany) was used to capture images. The relative density scores were calculated using ImageJ software (National Institutes of Health, Bethesda, MD, USA) on the basis of the mean fluorescence intensity (mean = IntDen/area), with background correction and normalization to the control group. Details regarding the western blot and qRT-PCR protocols are provided in the subsequent section, which focuses on the in vivo experiments.

Induction of Monocular FDM in Guinea Pigs

The Animal Care and Ethics Committee of Central South University (Changsha, China) approved the use of the animals in this study (2020sydw0224). The studies were conducted in accordance with the ARVO Statement for the Use of Animals in Ophthalmic and Vision Research. The experimental animals used in this study were Dunkin–Hartley guinea pigs obtained from Hunan Taiping Biotechnology Co., Ltd. (Hunan, China) and were housed in the Laboratory Animal Department of Central South University. The light level in the animal room was approximately 300 lux (12 hours of daylight and 12 hours of night); the room temperature was maintained at 24°C to 26°C, and the air humidity was 60%. All of the animals had access to sufficient food and clean drinking water. Because guinea pigs cannot synthesize vitamin C endogenously, they were provided with fresh vegetables twice daily as a vitamin C supplement.

Three-week-old guinea pigs (n = 42), each weighing approximately 150 to 180 g, were chosen for the study, with an equal number of males and females. The inclusion criteria for refractive error required bilateral spherical refractive errors greater than +1.00 diopter (D) and less than +1.50 D. Additionally, participants had to be free from ocular infections, cataracts, and fundus diseases. Monocular FDM was established by covering the right eye with a nontoxic, semitransparent mask made of latex balloons but leaving the left eye, both ears, mouth, and nose exposed. The tightness of the mask was adjusted according to the size of the guinea pig to prevent contact with the cornea and ensure normal feeding and activity. The ocular parameters of the guinea pigs were examined before and at the end of the treatment period.

Investigative Ophthalmology & Visual Science

Animal Experimental Paradigms

Research personnel were blinded throughout the study. To this end, the guinea pigs ($n = 42$) were randomly assigned to six groups, with assignments coded by an independent researcher. Different experimenters conducted pre- and post-experiment measurements without knowledge of the group assignments. The codes were revealed only after all the data had been collected and analyzed, ensuring unbiased results. The group assignments were as follows:

1. NC group—Normal (untreated) control group
2. Untreated FDM group—FDM-treated animals that were subjected to periocular saline injections without the following drug treatments
3. SKL group—FDM-treated animals that were subjected to periocular injections of the Wnt7b/β-catenin signaling pathway activator SKL2001 (8 mM)
4. TEP group—FDM-treated animals that were subjected to periocular injections of the Wnt7b/β-catenin signaling pathway inhibitor TEP (5 mM)
5. Glu group—FDM-treated animals that were subjected to periocular injections of the MMP-2 activator oxidized Glu (20 mg/mL)
6. ARP group—FDM-treated animals that underwent periocular injections of the MMP-2 inhibitor ARP-100 (5 mM)

In the FDM groups, the right eye (designated FDM-R) experienced form deprivation for 2 weeks, whereas the untreated left eye (designated FDM-L) served as an internal control. In the NC group, the right eye was designated NC-R, and the left eye was designated NC-L.

Drug stock solutions were prepared according to the manufacturer's recommendations. SKL, TEP, and ARP were initially dissolved in a vehicle containing 10% dimethyl sulfoxide (DMSO), 40% PEG300, 5% Tween 80, and 45% sterile saline. Glu was dissolved in sterile PBS. All drugs were diluted with physiological saline to the final working concentrations immediately before use. The experimental groups received a 10-µL periocular injection of the assigned drug on days 1, 4, 7, 10, and 13 during the deprivation period, with injections administered between 11:00 AM and 1:00 PM. Injections were administered into the peribulbar space of the right eye on the temporal side, with a needle insertion depth of approximately 2 to 3 mm.

Analysis of Refraction and AL

Before FDM induction, baseline ocular parameters, including the AL and refractive errors of both eyes, were measured across all experimental groups. The statistical analysis revealed no significant differences in any parameter between the groups ($P > 0.05$), confirming that the groups were comparable at the beginning of the study. The refractive errors of the guinea pigs were measured using an eccentric infrared photorefractor (Striatech, Tübingen, Germany).[26,27] The accompanying software automatically calculates the refractive error in the vertical meridian. Measurements were made in a dark room without anesthesia or cycloplegia. Refractions were recorded when the Purkinje image was centered in the pupil of the guinea pig, and the pupil diameter and refractive error were relatively stable. Five consecutive measurements were recorded for each eye, and the average value was calculated. The power refractor used in this study has a manufacturer-specified accuracy of ±0.25 D.

AL measurements were conducted using an A-scan ultrasound unit (Axis Nano; Quantel Medical, Cournon-d'Auvergne, France) with modifications to adapt the probe for guinea pig eyes.[26] Specifically, a plastic tube approximately 8 mm in length and 3 mm in diameter was attached to the front end of the probe as a stand-off device. The tube was filled with double-distilled water and sealed with parafilm (Amcor, Victoria, Australia).

For the measurements, guinea pigs were placed in a quiet environment, and one or two drops of 0.5% proparacaine hydrochloride (H20160133; Alcon, Geneva, Switzerland) were applied to the cornea for local anesthesia. The tip of the stand-off tube was pre-moistened with saline and gently positioned on the apex of the anterior corneal surface, ensuring perpendicular contact to minimize measurement errors. The A-scan ultrasound unit operated at a frequency of 10 MHz, offering a resolution of approximately 0.01 mm. Each measurement was repeated 10 times, and the mean value was recorded, with the standard deviation controlled within 0.1 mm to ensure accuracy and consistency.

Quantitative Real-Time PCR

On day 14 of the experiment, the guinea pigs were humanely euthanized via an intraperitoneal injection of an overdose of pentobarbital sodium (150 mg/kg). The eyes were carefully dissected, and the scleral tissue was precisely sectioned along the sagittal plane using the optic nerve as an anatomical reference to ensure unbiased sample allocation. The optic nerve head (ONH) was excised to prevent potential confounding influences of its unique structure on downstream analyses. The resulting scleral halves were labeled "left" and "right." A computer-generated randomization algorithm (the RAND function in Microsoft Excel) was used to assign each half for either qRT-PCR or WB analysis. The half designated for qRT-PCR was placed in TRIzol (Life Technologies, Carlsbad, CA, USA) and homogenized with a cryogenic grinder. HFSFs were homogenized using ultrasonication in TRIzol Reagent. The TRIzol Reagent was used to extract RNA from the sclerae or cells according to the manufacturer's guidelines. After the RNA concentration was determined with a NanoDrop spectrophotometer (NanoDrop Technologies, Wilmington, DE, USA) to be within the 200- to 1000-ng/µL range, reverse transcription was conducted to synthesize cDNA using a reverse transcription kit (R20613; TransGen Biotech, Beijing, China). With specific primers and SYBR Green (Q20421; TransGen Biotech), qRT-PCR was performed on a QuantStudio 7 Flex Real-Time PCR System (Thermo Fisher Scientific, Waltham, MA, USA). With threshold cycle values and the $2^{-\Delta\Delta Ct}$ method, the MMP-2 mRNA and collagen I mRNA levels were estimated by normalization to those of glyceraldehyde 3-phosphate dehydrogenase (GAPDH) mRNA. The Table lists the sequences of the primers used.

Immunoblot Analysis

The other half of the dissected sclera was homogenized in radioimmunoprecipitation assay (RIPA) lysis buffer (P105; Beyotime, Jiangsu, China) supplemented with 1/100 protease inhibitor cocktail (P0013B; Beyotime). HFSFs were homogenized in the same lysis buffer. The homogenates were subjected to 15 minutes of centrifugation at 12,000*g* at 4°C to extract the supernatants. Protein concentrations were measured using an Enhanced BCA protein assay kit (P0010; Beyotime).

Table. Primers for qRT-PCR

Gene	Forward Primer	Reverse Primer
hcollagen I	GAGGGCCAAGACGAAGACATC	CAGATCACGTCATCGCACAAC
hMMP-2	TACAGGATCATTGGCTACACACC	GGTCACATCGCTCCAGACT
hGAPDH	GGAGCGAGATCCCTCCAAAAT	GGCTGTTGTCATACTTCTCATGG
gcollagen I	AAGTCCTCTTCCGCCCATTG	TATGCCTTTTGGGGCGACTT
gMMP-2	GGTACCCGTTCGATGGGAAG	CCCAGAGTCCACAGCTCATC
gGAPDH	TTCTACCCACGGCAAGTTCC	CCAGCATCACCCCACTTGAT

Note: "h" represents human and "g" represents guinea pig.

Equal amounts of 15 µg of total protein from HFSFs or 30 µg of total protein from guinea pig scleral samples were loaded onto 4% to 20% SurePAGE gels (M00656; GenScript, Piscataway, NJ, USA), separated by electrophoresis, and then blotted onto nitrocellulose membranes (MilliporeSigma, Billerica, MA, USA). The membranes were blocked with 5% nonfat milk (BS102; Biosharp) for 2 hours at room temperature. Afterward, the membranes were incubated with primary antibodies against collagen I (ab138492 and ab270993; Abcam,), MMP-2 (ab92536; Abcam), Wnt7b (ab227607; Abcam), or GAPDH (AF2823; Beyotime) overnight at 4°C. After three 5-minute washes with 1× Tris-buffered saline with Tween 20 (TBST, BL315B; Biosharp), the membranes were incubated with Goat Anti-Rabbit IgG (H+L)–HRP Conjugate (A0208; Beyotime) for 2 hours at room temperature. The membranes were subjected to three 5-minute washes with 1× TBST, and a ChemiDoc MP Imaging System (Bio-Rad, Hercules, CA, USA) was used to visualize the protein bands. ImageJ software was used to analyze the protein band intensities. For statistical analysis and normalization, GAPDH was used as an internal control.

AFM Mechanical Measurements

The mechanical properties of HFSFs and sclerae were characterized via AFM (MFP-3D; Asylum Research, Santa Barbara, CA, USA) with a colloidal probe.[20,28] The AFM instrument was attached to an inverted microscope (IX71; Olympus, Tokyo, Japan) featuring an electron-multiplying charge-coupled device camera (Ixon3X; Andor Technology, Belfast, Ireland) for simultaneous recording of mechanical and optical data. The colloidal probes for measuring the sclera and HFSFs were composed of glass beads with $R \cong 25$ µm and $R \cong 15$ µm adhered to the front end of rectangular cantilevers with elastic constants of 0.3 N/m (NSC35/Pt; MikroMasch, Sofia, Bulgaria) and 0.09 N/m (NSC36/Pt; MikroMasch), respectively. A thin coating of poly(L-lysine)-g-poly(ethylene glycol) (PLL-g-PEG) was deposited on the colloidal probe before the AFM measurements, which significantly reduced the surface adherence of the sclera and the HFSFs to the probe.[28] The AFM closed fluid chamber housed either the sclera or HFSFs at the bottom, with the AFM cantilever positioned to contact the top surface of the samples. The force measurements for the sclera were taken at room temperature (25°C), whereas those for HFSFs were conducted at 37°C, which was monitored and maintained by a local temperature controller inside the fluid chamber.

The elastic modulus E for both the sclera and HFSFs was determined through force indentation measurements using AFM in contact mode. The indentation force, $F(\delta)$, was recorded as a function of indentation δ when the AFM probe was initially pressed down against the sample surface at a constant loading speed of $v = 50$ µm/s (approach) and then retracted from the cell surface at the same speed. With 1- to 3-µm indentation depths, the approaching curves were fitted using the Hertz model, $F = \frac{4}{3(1-\upsilon^2)} E R^{0.5} \delta^{1.5}$, to calculate E,[27] where $\upsilon \cong 0.33$ is Poisson's ratio. The elastic modulus of the sclera was measured at 20 distinct locations and was distributed as evenly as possible across the tested region. These locations included areas 2 to 4 mm proximal to the ONH margin and extended toward the equatorial zone. Each location was measured at least three times. Similarly, for each experimental group of cells, the elastic modulus of at least 20 cells was measured, with each cell subjected to a minimum of three force indentation measurements.

Statistical Analysis

All of the statistical analyses were carried out with Prism 8.0.2 (GraphPad, Boston, MA, USA). The experimental results are displayed as mean ± SEM. The raw data were processed and graphs were created using GraphPad Prism. The outliers were identified and removed through the ROUT method ($Q = 1\%$). Normality was evaluated with the Shapiro–Wilk test, whereas Levene's test was used to assess homogeneity of variance. When the data met the assumptions of normality and homogeneity of variance, unpaired two-sided Student's t-tests were used to assess differences between the treated (right) eyes of the two groups. One-way ANOVA was utilized for comparisons involving three or more groups. If the above assumptions were not fulfilled, nonparametric tests were applied (Mann–Whitney U test or Kruskal–Wallis test). The group sizes were determined via a power analysis (power = 0.8, alpha = 0.05) using estimated effect sizes from preliminary data. $P < 0.05$ was considered statistically significant ($^*P < 0.05$, $^{**}P < 0.01$, $^{***}P < 0.001$, $^{****}P < 0.0001$).

Results

Effects of MMP-2 on the Expression of Collagen I in HFSFs

Glu is an agonist and ARP is an inhibitor of MMP-2.[29,30] We used a Cell Counting Kit-8 (CCK-8) assay to evaluate their effects. Both Glu and ARP had concentration-dependent cytotoxic effects on HFSFs, with half-maximal inhibitory concentration (IC_{50}) values of 2.447 mg/mL and 13.86 nM at 24 hours, respectively (Supplementary Figs. S1, S2). The fluorescence intensity of MMP-2 was also significantly increased in the HFSFs treated with Glu, as visualized by IF staining, but it was notably decreased in the HFSFs treated with ARP. The fluorescence intensity of MMP-2 in the HFSFs treated with Glu was 2.09 times greater than that in the HFSFs treated with ARP (Figs. 1A, 1B). Additionally, the MMP-2

Investigative Ophthalmology & Visual Science

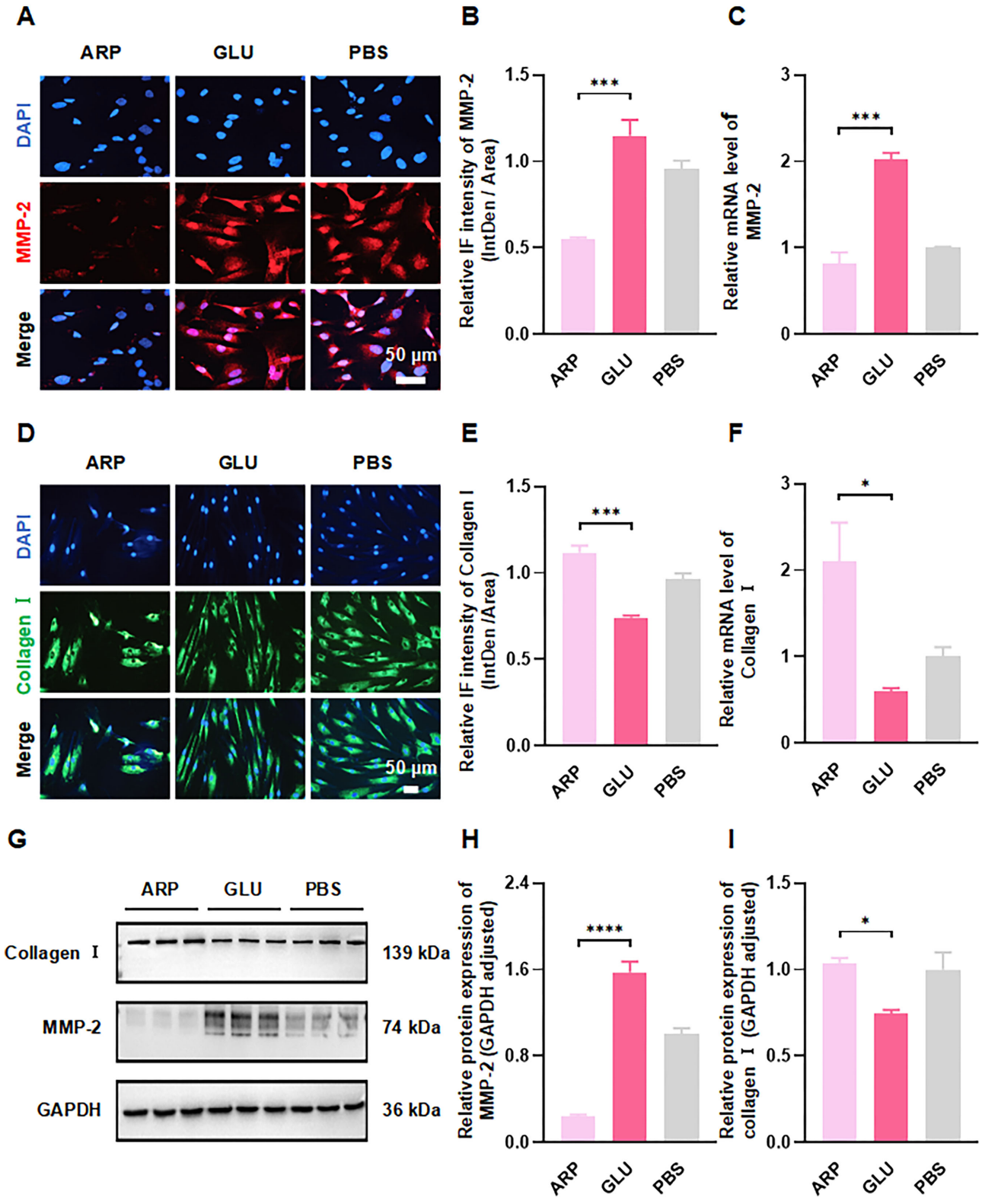

Figure 1. MMP-2 promotes the degradation of collagen I in HFSFs. (**A, B**) Representative images of IF staining and the corresponding relative IF intensity of MMP-2 in HFSFs treated with Glu, ARP, or PBS for 24 hours. *Blue* indicates DAPI; *red*, MMP-2. *Scale bar*: 50 µm. (**C**) The mRNA levels of MMP-2 in the HFSFs treated with Glu, ARP, or PBS for 24 hours were measured via qRT-PCR. GAPDH was used as an internal control. (**D, E**) Representative images of IF staining and the relative IF intensity of collagen I in HFSFs treated with Glu, ARP, or PBS for 24 hours. *Blue* indicates DAPI; *green*, collagen I. *Scale bar*: 50 µm. (**F**) The mRNA levels of collagen I in the HFSFs treated with Glu, ARP, or PBS for 24 hours were measured via qRT-PCR. GAPDH was used as an internal control. (**G–I**) WB analysis of MMP-2 and collagen I expression in HFSFs following treatment with ARP, Glu, or PBS for 24 hours. The data are presented as mean ± SEM. The statistical significance of differences between the two groups was calculated via one-way ANOVA. $^{*}P < 0.05$, $^{***}P < 0.001$, $^{****}P < 0.0001$.

Investigative Ophthalmology & Visual Science

mRNA level in the HFSFs treated with Glu was 2.46 times greater than that in the ARP-treated HFSFs (Fig. 1C). These results confirmed that Glu and ARP can regulate MMP-2 expression in HFSFs.

We evaluated collagen I expression in HFSFs by manipulating MMP-2 levels to investigate the potential effect on collagen I regulation. Initially, IF analysis revealed a notable increase in collagen I fluorescence intensity in the HFSFs treated with ARP, whereas a reduction in collagen I fluorescence intensity was found in the HFSFs treated with Glu (Figs. 1D, 1E). Additionally, qRT-PCR revealed a 3.48-fold increase in collagen I transcript levels in the HFSFs treated with ARP compared with those in the HFSFs treated with Glu (Fig. 1F). Moreover, WB analysis revealed a link between elevated MMP-2 levels and decreased collagen I levels (Fig. 1G). Specifically, the MMP-2 protein level increased by 6.6-fold, whereas the collagen I level decreased by 30% in the HFSFs treated with Glu compared with those treated with ARP (Figs. 1H, 1I). In summary, these findings indicate that MMP-2 promotes collagen I degradation in HFSFs.

Effects of the Wnt7b/β-Catenin Signaling Pathway on the Expression of MMP-2 and Collagen I in HFSFs

SKL is an agonist and TEP is an inhibitor of the Wnt7b/β-catenin signaling pathway,[31,32] with IC_{50} values of 71.38 µM and 50.07 µM, respectively, in HFSFs after 24 hours of treatment, as shown by CCK-8 assays. These IC_{50} values were subsequently applied as treatment concentrations in the cell-based experiments (Supplementary Figs. S1, S2). Wnt7b is a hallmark of Wnt7b/β-catenin signaling pathway activation.[33] The effects of SKL and TEP on the expression of Wnt7b were then explored via WB analysis (Fig. 2A). We found a notable 1.5-fold increase in Wnt7b expression in the HFSFs treated with SKL compared with the HFSFs treated with PBS. Conversely, treatment with TEP resulted in a 63% reduction in Wnt7b levels in the HFSFs compared with those in the PBS-treated cells (Fig. 2B). These findings confirm that SKL and TEP can modulate the activation of the Wnt7b/β-catenin signaling pathway in HFSFs.

Next, we elucidated the underlying associations between the activation of the Wnt7b/β-catenin signaling pathway and the expression of MMP-2 and collagen I. We directly quantified the expression of MMP-2 and collagen I after manipulating the activity of the Wnt7b/β-catenin signaling pathway. WB analysis revealed a 1.21-fold increase in MMP-2 expression and a 12% decrease in collagen I levels in the HFSFs subjected to SKL treatment compared with those in the HFSFs treated with PBS. Conversely, the TEP-treated cells exhibited a 73% reduction in MMP-2 expression but a 3.23-fold increase in collagen I expression (Fig. 2B). IF experiments further revealed that MMP-2 expression increased but collagen I expression decreased in the HFSFs treated with SKL and that MMP-2 expression decreased but collagen I expression increased in the HFSFs treated with TEP (Figs. 2C–2F). Moreover, qRT-PCR revealed that the expression of the MMP-2 transcript increased 3.08-fold and that of collagen I decreased 4.27-fold in the HFSFs treated with SKL compared with those treated with TEP (Fig. 2G). These findings indicate that activation of the Wnt7b/β-catenin signaling pathway results in the upregulation of MMP-2 and a reduction in collagen I expression.

Effects of the Wnt7b/β-Catenin Signaling Pathway or MMP-2 on the Elastic Modulus of HFSFs

Because the elastic modulus is an essential indicator of mechanical properties and is closely related to the physiological activity and health of cells,[21,34] we used AFM with a colloidal probe to measure the elastic modulus of HFSFs (Figs. 3A, 3B). The elastic modulus of the HFSFs treated with TEP was 3.14 times greater than that of the HFSFs treated with SKL. Moreover, the elastic modulus of the HFSFs treated with ARP was 1.38 times greater than that of the HFSFs treated with Glu (Fig. 3C). The results indicate that both the activation of the Wnt7b/β-catenin signaling pathway and the upregulation of MMP-2 increased the degradation of collagen I and reduced the elastic modulus of HFSFs.

Effects of MMP-2 on Refraction and the AL of Guinea Pigs With FDM

An FDM guinea pig model was generated to further study the roles of MMP-2 and the Wnt7b/β-catenin signaling pathway in the development of myopia (Fig. 4A).[16] First, the refractive error of the FDM-R group became relatively myopic by approximately –2.64 D, whereas the refractive errors of the NC-R group remained relatively constant. Second, the AL elongation in the FDM-R eyes was 4.2 times greater than that in the NC-R eyes (Figs. 4B, 4C), indicating successful form deprivation in the guinea pig eyes. Additionally, the scleral expression of the MMP-2 protein in the untreated FDM group was increased by approximately 79.29% compared with that in the NC group, whereas collagen I protein expression was decreased by approximately 31.48% in the untreated FDM group compared with that in the NC group (Figs. 4D–4F). These findings suggest that form-deprivation myopia results in the upregulation of MMP-2 expression and the downregulation of collagen I expression in the sclera.

Glu or ARP was administered via peribulbar injection to the FD eyes of guinea pigs on days 1, 4, 7, 10, and 13 to determine how MMP-2 expression influences the severity of myopia. Western blot analysis revealed that MMP-2 protein expression in the Glu-treated group was approximately 1.48-fold higher than that in the ARP-treated group and 1.20-fold higher than that in the untreated FDM group, whereas MMP-2 protein expression in the ARP-treated group was approximately 0.82-fold of that in the untreated FDM group (Figs. 4D, 4E).These results indicate that both Glu and ARP altered MMP-2 expression in the sclera of the FDM-affected guinea pigs. Additionally, the MMP-2 mRNA levels in the Glu-injected guinea pigs were 7.37 times greater than those in the ARP-treated guinea pigs and 1.53 times greater than those in the untreated guinea pigs with FDM, whereas the MMP-2 mRNA level in the ARP-treated guinea pigs was approximately 0.21 times that in the untreated guinea pigs in the FDM group (Fig. 4G). Similarly, collagen I mRNA expression in the Glu-treated group was approximately 0.28 times that in the ARP-treated group and 0.39 times that in the untreated FDM group, with collagen I mRNA levels in the ARP-treated group being approximately 1.36 times greater than those in the untreated FDM group (Fig. 4G). These results suggest that both the activation and inhibition of MMP-2 significantly influence the progression of form-deprivation myopia. Furthermore, we found a close correlation between increased scleral MMP-2 expression and decreased collagen I expression during myopia development. Additionally, the WB and qRT-PCR results indicate that

Investigative Ophthalmology & Visual Science

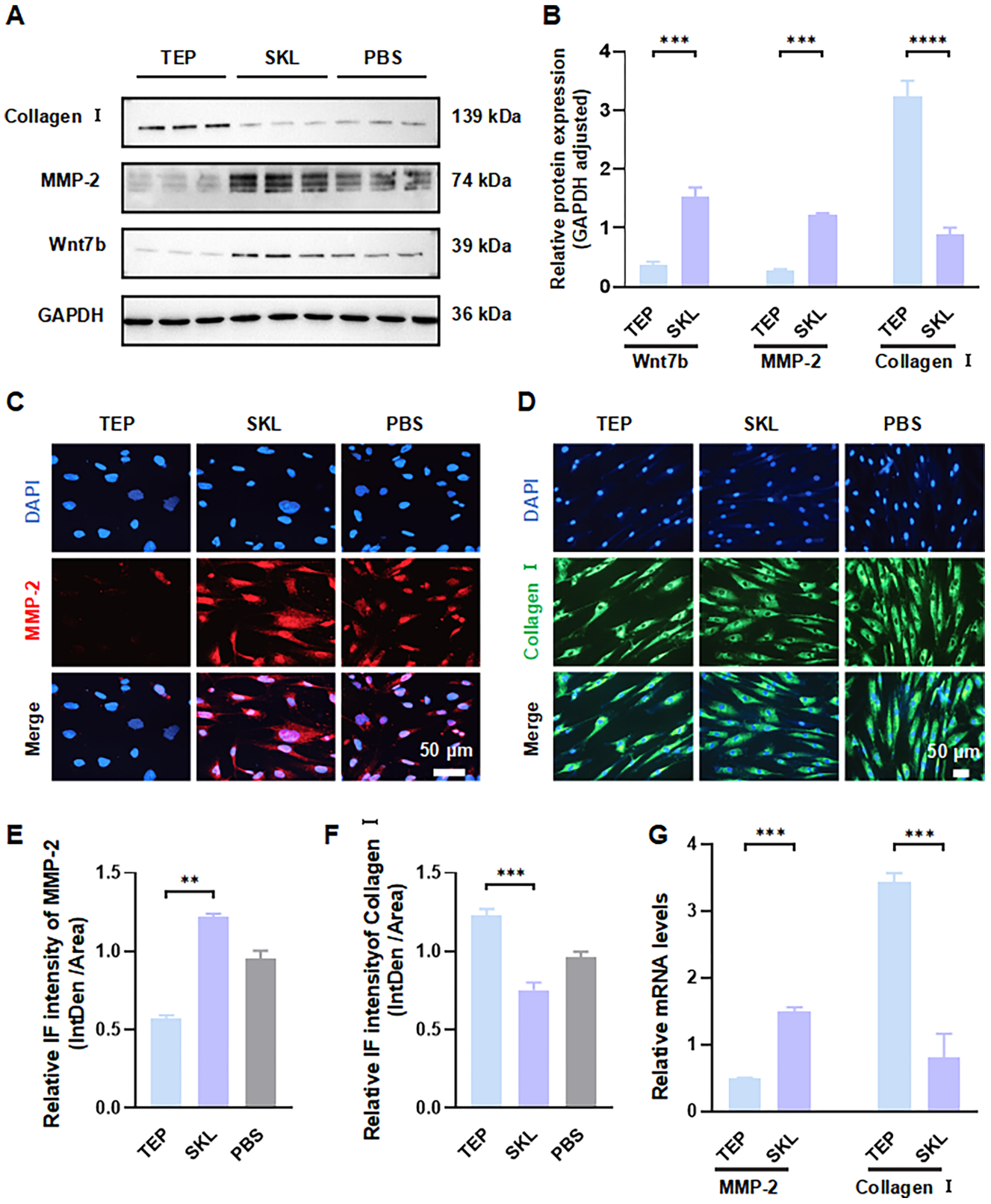

Figure 2. Effects of the Wnt7b/β-catenin signaling pathway on the expression of MMP-2 and the metabolism of collagen I in HFSFs. (**A**) The expression of Wnt7b, MMP-2, and collagen I in the HFSFs treated with TEP, SKL, or PBS was determined by WB analysis. (**B**) Densitometric quantification of the WB results for Wnt7b, MMP-2, and collagen I. (**C**) The protein expression levels of MMP-2 in the HFSFs treated with TEP, SKL, or PBS were determined by IF staining. *Blue* indicates DAPI; *red*, MMP-2. *Scale bar*: 50 μm. (**D**) The protein expression levels of collagen I in the HFSFs treated with TEP, SKL, or PBS were determined by IF staining. *Blue* indicates DAPI; *green*, collagen I. *Scale bar*: 50 μm. (**E**) Relative IF intensity of MMP-2. (**F**) Relative IF intensity collagen I. (**G**) The mRNA levels of MMP-2 and collagen I were analyzed by qRT-PCR with specific primers. GAPDH was used as an internal control. The data are presented as mean ± SEM. The statistical significance of differences between two groups was calculated via one-way ANOVA. $^{**}P < 0.01$, $^{***}P < 0.001$, $^{****}P < 0.0001$.

Investigative Ophthalmology & Visual Science

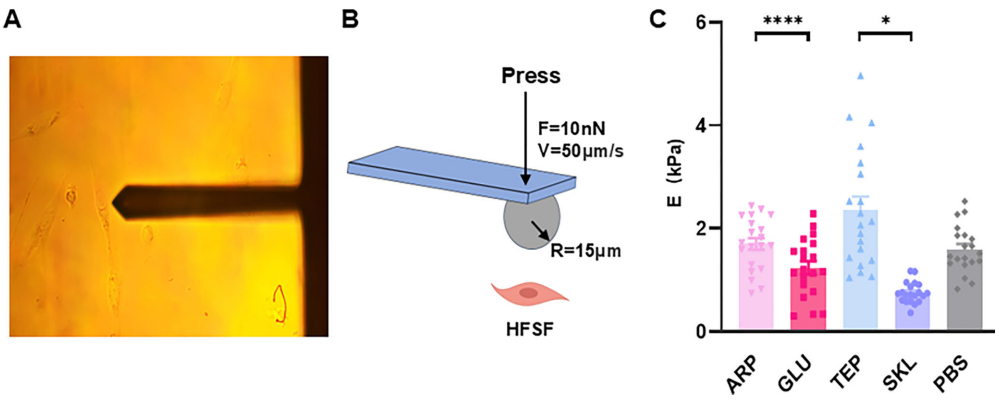

Figure 3. The Wnt7b/β-catenin signaling pathway influences the elastic modulus (*E*) of HFSFs. (**A**) Real-time top view of the AFM measurement of HFSFs. (**B**) Schematic diagram of AFM measurements of the elastic modulus of HFSFs using colloidal probes. (**C**) Statistical analysis of the elastic modulus of HFSFs in the SKL, TEP, Glu, ARP, and PBS groups. The data are presented as mean ± SEM. The statistical significance of differences between the two groups was calculated via one-way ANOVA. *$P < 0.05$ and ****$P < 0.0001$.

the upregulation of MMP-2 and downregulation of collagen I induced by form deprivation, compared with those in the NC group, are difficult to reverse with MMP-2 inhibitors alone.

Compared with the guinea pigs injected with ARP, the guinea pigs injected with Glu presented a 1.76-fold increase in relative myopia, along with a 1.78-fold increase in AL (Figs. 4H, 4I). These results suggest that MMP-2 is involved in the development of myopia by promoting the degradation of collagen I and thereby axial ocular elongation and a myopic shift in refractive error.

Effects of the Wnt7b/β-Catenin Signaling Pathway on Refraction and the AL of Guinea Pigs With FDM

We manipulated the activation of the Wnt7b/β-catenin pathway in the sclera of guinea pigs with FDM and subsequently measured the MMP-2 and collagen I expression levels to determine whether the Wnt7b/β-catenin signaling pathway influences myopia development by regulating MMP-2 expression in myopic eyes. WB analysis revealed that the scleral Wnt7b protein level in the SKL-treated guinea pigs was 2.53 times greater than that in the guinea pigs treated with TEP and 1.38 times greater than that in the untreated guinea pigs with FDM. Scleral Wnt7b protein levels in the untreated guinea pigs with FDM were 1.83 times higher than those in the guinea pigs injected with TEP (Figs. 5A–5C).

Furthermore, WB analysis revealed that the scleral MMP-2 protein level in the SKL-treated guinea pigs was 3.35 times greater than that in the guinea pigs treated with TEP and 1.54 times greater than that in untreated guinea pigs with FDM. The MMP-2 protein level in the untreated FDM group was 2.17 times greater than that in the TEP group (Figs. 5A, 5C). However, scleral collagen I protein levels in the TEP-treated guinea pigs were 1.9 times greater than those in the SKL-treated guinea pigs and 1.2 times greater than those in the untreated guinea pigs with FDM. The collagen I protein level in the untreated guinea pigs with FDM was 1.57 times greater than that in the SKL-treated guinea pigs (Figs. 5A, 5C). Consistent with the WB results, scleral MMP-2 mRNA levels in the SKL-treated guinea pigs were 2.35 times greater than those in the TEP-treated guinea pigs and 1.66 times greater than those in the untreated guinea pigs with FDM. The MMP-2 mRNA level in the untreated guinea pigs with FDM was 1.42 times greater than that in the TEP-treated guinea pigs. Additionally, scleral collagen I mRNA levels in the TEP-treated guinea pigs were 2.38 times greater than those in the SKL-treated guinea pigs and 1.51 times greater than those in the untreated guinea pigs with FDM. Collagen I mRNA levels in the untreated guinea pigs in the FDM group were 1.59 times higher than those in the SKL-treated guinea pigs (Fig. 5D).

These findings suggest that Wnt7b/β-catenin signaling promotes the degradation of collagen I in the sclera by upregulating MMP-2 expression, thus contributing to scleral remodeling in guinea pigs. However, both the WB and qRT-PCR results indicate that inhibitors of the Wnt7b/β-catenin signaling pathway could not fully inhibit the upregulation of MMP-2 and the downregulation of collagen I associated with form-deprivation myopia compared with the levels in the NCs.

Finally, refraction and AL measurements indicated that, compared with the TEP-treated guinea pigs, the SKL-treated guinea pigs exhibited refractive errors that were 1.85 times greater and ALs that were 1.62 times longer (Figs. 5E, 5F). These results indicate that activation of the Wnt7b/β-catenin signaling pathway induces increased myopic shifts in refractive error.

Effects of the Wnt7b/β-Catenin Signaling Pathway or MMP-2 on the Elastic Modulus of the Sclera in Guinea Pigs With FDM

We evaluated the mechanical properties of the scleras of myopic eyes using AFM with a colloidal probe to measure the scleral elastic modulus (Figs. 6A, 6B). The results revealed a significant reduction in the scleral elastic modulus across all five FDM groups after the development of myopia compared with that in the NC group, indicating that myopia reduced scleral stiffness (Fig. 6C). Among the five FDM groups, the scleral elastic modulus of the guinea pigs injected with TEP was 3.48 times greater than that of the guinea pigs injected with SKL and 1.49 times greater than that of the untreated guinea pigs with FDM. Furthermore, compared with the SKL group, the untreated FDM group presented a 2.20-fold greater elastic modulus. Similarly, the

Investigative Ophthalmology & Visual Science

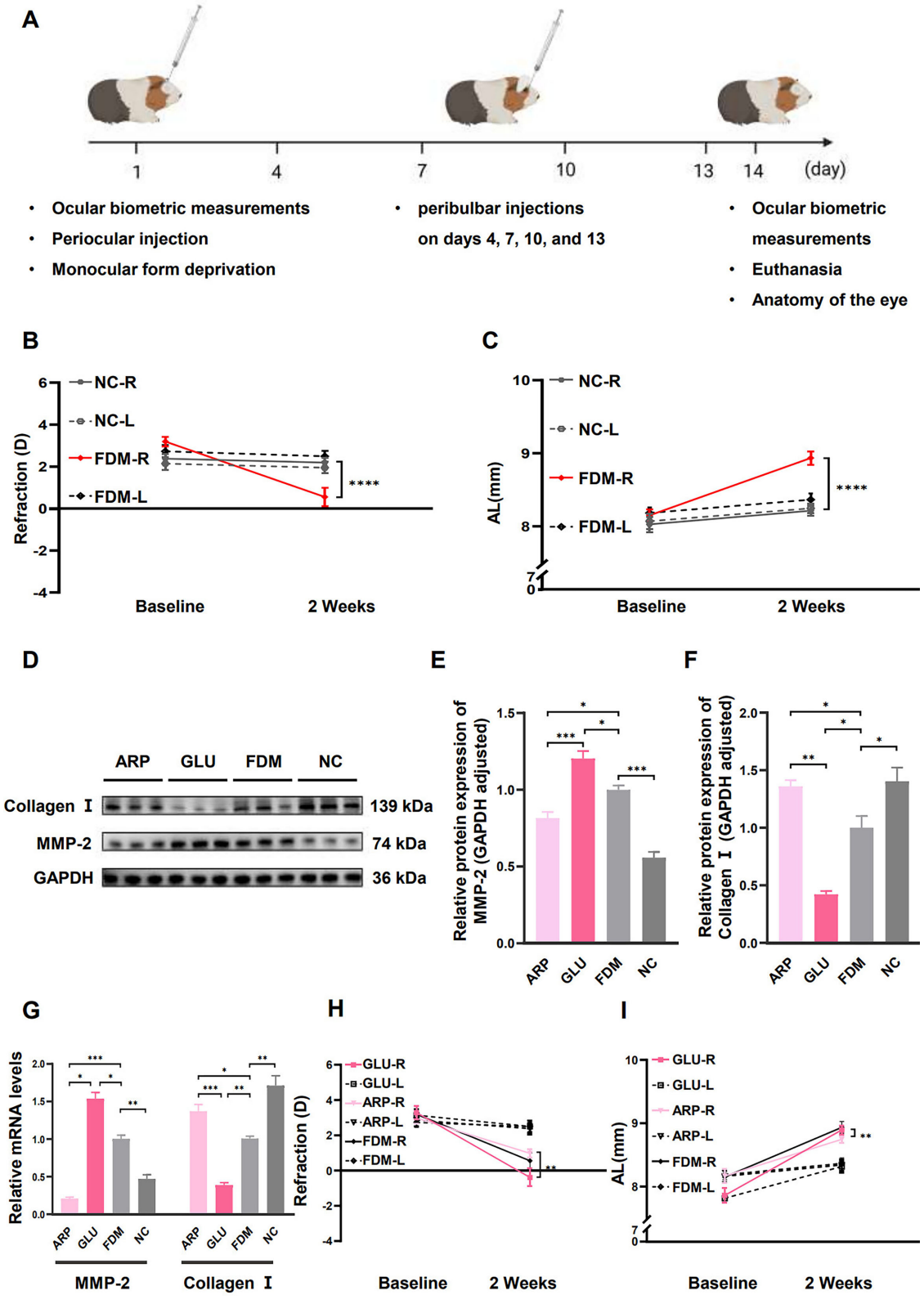

Figure 4. Effects of MMP-2 on the refraction and AL of guinea pigs with FDM that were treated for 2 weeks. (**A**) Diagrammatic representation of the in vivo experiments. (**B**) Refractions observed after 2 weeks of NC and FDM treatment. (**C**) ALs of the NC and FDM groups after 2 weeks. (**D**) The protein levels of MMP-2 and collagen I in the sclera of the ARP, Glu, FDM, and NC groups were determined by WB analysis. (**E, F**) Densitometric quantification of the WB results for MMP-2 (**E**) and collagen I (**F**). (**G**) The scleral mRNA levels of MMP-2 and collagen I were analyzed by qRT-PCR with specific primers. GAPDH was used as an internal control. (**H**) Refractive errors measured before and after 2 weeks of Glu and ARP treatment. (**I**) AL was measured before and after 2 weeks of Glu and ARP treatment. The data are presented as mean ± SEM. The statistical significance of differences between two groups was calculated via one-way ANOVA. $^{*}P < 0.05$, $^{**}P < 0.01$, $^{***}P < 0.001$, $^{****}P < 0.0001$.

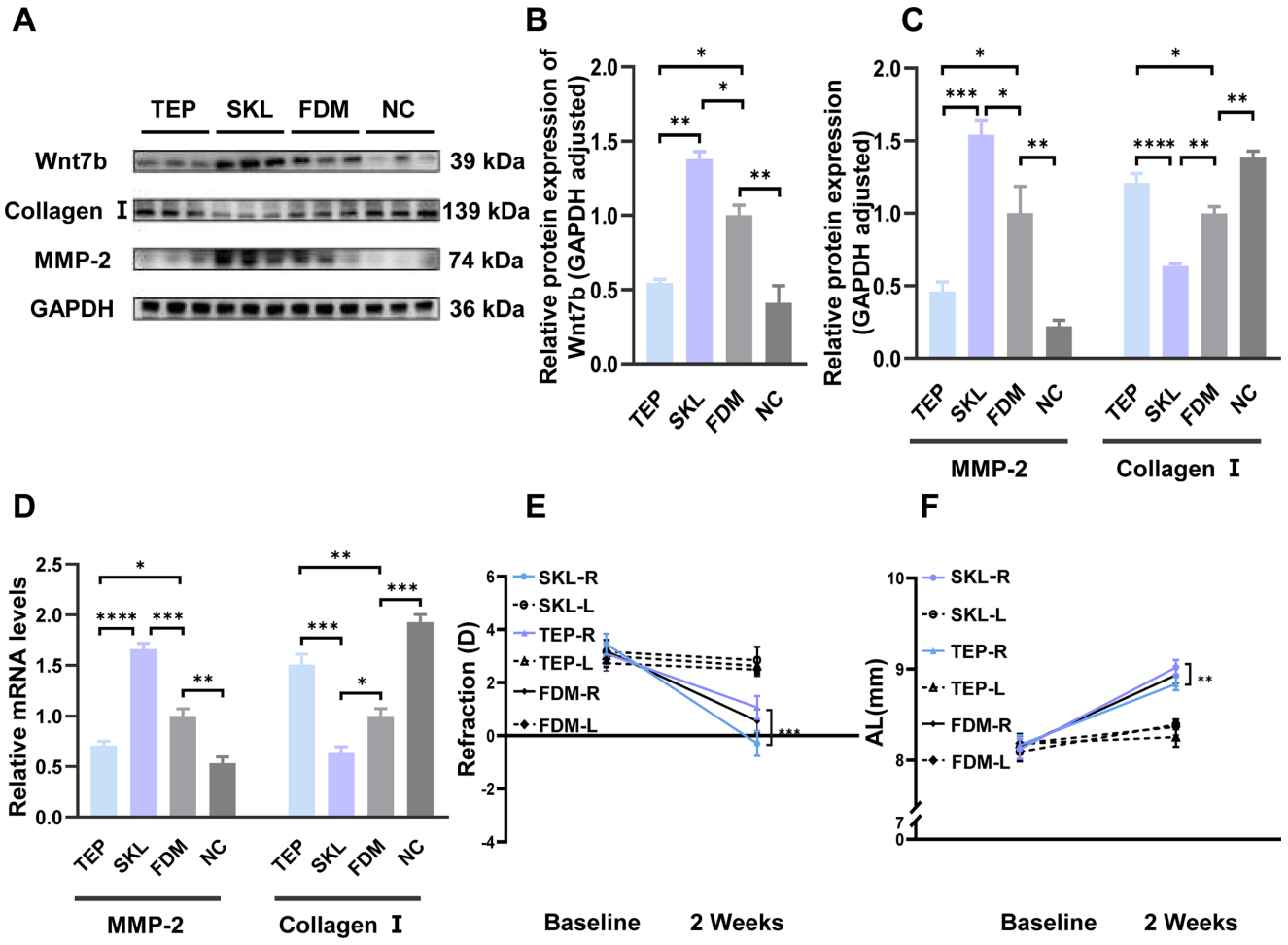

Figure 5. Effects of the Wnt7b/β-catenin signaling pathway on refraction and the AL of guinea pigs with FDM. (**A**) The protein levels of Wnt7b, MMP-2, and collagen I in the sclera of the ARP, Glu, FDM, and NC groups were determined by WB analysis. (**B, C**) Densitometric quantification of the WB results for Wnt7b (**B**) and for MMP-2 and collagen I (**C**). (**D**) The scleral MMP-2 and collagen I mRNA levels were analyzed by qRT-PCR with specific primers. GAPDH was used as an internal control. (**E**) Refractive errors were measured before and after 2 weeks of SKL or TEP treatment. (**F**) AL was measured before and after 2 weeks of SKL or TEP treatment. The data are presented as mean ± SEM. The statistical significance of differences between two groups was calculated via one-way ANOVA. $^{*}P < 0.05$, $^{**}P < 0.01$, $^{***}P < 0.001$, $^{****}P < 0.0001$.

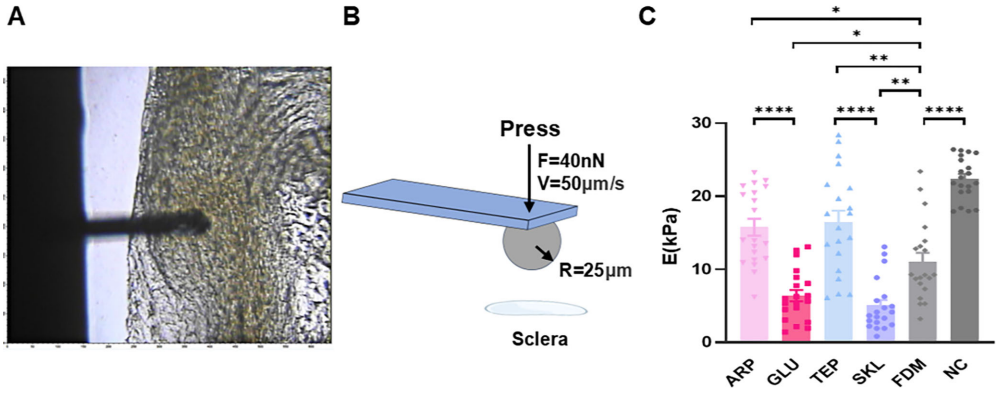

Figure 6. Effects of SKL, TEP, Glu, and ARP on the elastic modulus (*E*) of the sclera. (**A**) Real-time top view of an AFM measurement of the sclera. (**B**) Schematic diagram of the AFM measurement of the elastic modulus of the sclera using colloidal probes. (**C**) Statistical analysis of the elastic modulus of the sclera in the SKL, TEP, Glu, ARP, FDM, and NC groups. $^{*}P < 0.05$, $^{**}P < 0.01$, $^{****}P < 0.0001$ (one-way ANOVA). The data are presented as mean ± SEM.

Investigative Ophthalmology & Visual Science

scleral elastic modulus in the guinea pigs injected with ARP was 2.47 times greater than that in the Glu-treated group and 1.43 times greater than that in the untreated guinea pigs with FDM, with the modulus in the untreated FDM group being 1.73-fold greater than that in the Glu-treated group (Fig. 6C). These findings indicate that, during scleral remodeling in myopia, activation of the Wnt7b/β-catenin signaling pathway and upregulation of MMP-2 expression substantially decrease the scleral elastic modulus, thus facilitating myopia progression. Conversely, inhibiting Wnt7b/β-catenin signaling or downregulating MMP-2 expression attenuates this effect, potentially slowing the progression of myopia.

Discussion

Role of MMP-2 in Collagen I Degradation

Previous reports have shown that MMP-2 disrupts the balance between ECM production and degradation in the sclera, thereby inducing scleral remodeling during the development of myopia.[13,35,36] Collagen I is the main component of the scleral ECM. MMP-2 plays a key role in the degradation of collagen I in the sclera.[24] Previous experimental myopia models have shown that elevated MMP-2 expression in the sclera accelerates collagen I degradation.[16] In our current study, upregulation of MMP-2 expression in HFSFs not only led to a reduction in collagen I levels but also decreased the elastic modulus. This finding is consistent with previous findings by Wu et al.,[16] who reported a similar relationship between MMP-2 and collagen I in related cell and animal models. In guinea pigs with FDM, the upregulation of MMP-2 expression leads to a decrease in collagen I and the elastic modulus in the sclera, resulting in axial elongation and myopic shift. These results confirm that MMP-2 can mediate collagen I degradation and promote scleral remodeling and the development of myopia. Because collagen proteins are integral to the structure and biomechanical properties of the sclera,[23] the reduction in total scleral collagen, together with the altered morphology and arrangement of collagen fibers, leads to a decrease in scleral stiffness, with increased axial elongation and myopic shifts in refractive error being the in vivo expression of the same.[24,25]

Regulatory Role of the Wnt7b/β-Catenin Signaling Pathway in Myopia

The Wnt/β-catenin signaling pathway has been reported to play an important role in the development of myopia. Multiple studies, including those that explored this pathway in human samples,[17] those that investigated the molecular mechanisms in animal models,[18,37] and those that focused on genetic aspects, have provided evidence for this role. Wnt7b, a critical ligand in the Wnt/β-catenin signaling pathway, is closely associated with high myopia.[19,38,39] The Wnt/β-catenin pathway consists of extracellular signals, membrane segments, cytoplasmic segments, and nuclear segments. Matrix metalloproteinases have been identified as downstream target genes of the nuclear segment.[40] Among the matrix metalloproteinase family, MMP-2 is strongly associated with the development of myopia.[41–43] In this study, we found that the activation or inhibition of the Wnt7b/β-catenin signaling pathway significantly upregulated or downregulated the expression of MMP-2 in HFSFs, respectively. This change in MMP-2 expression promoted or inhibited the degradation of collagen I, thereby causing changes in the elastic modulus of HFSFs. In the FDM model of guinea pigs, activation of the Wnt7b/β-catenin pathway in the sclera resulted in the upregulation of MMP-2 expression. This upregulation led to accelerated collagen I degradation and reduced scleral stiffness. As a result, axial elongation and myopia progression both increased. Conversely, when the Wnt7b/β-catenin pathway was inhibited, the expression of MMP-2 was downregulated, collagen I degradation was reduced, and scleral stiffness was increased. Thus, the progression of myopia has slowed. These results highlight the critical role of the Wnt7b/β-catenin signaling pathway in modulating scleral biomechanics during myopia development. Scleral remodeling is a dynamic process involving continuous synthesis and degradation of the ECM.[24] During normal eye development, ECM accumulation and collagen I synthesis contribute to increased scleral stiffness, which helps maintain structural integrity and refractive error stability during puberty and early adulthood.[23] Our findings suggest that activation of the Wnt7b/β-catenin pathway accelerates collagen I degradation, which reduces scleral stiffness and promotes abnormal scleral remodeling in myopic eyes, leading to increased axial elongation and further myopia progression. Thus, our results confirm that Wnt7b/β-catenin signaling regulates scleral remodeling by modulating MMP-2 expression and collagen I degradation, contributing to myopia progression.

Crucial Role of Biomechanics of HFSFs and the Sclera During Myopia Progression

Scleral fibroblasts are the primary cellular component of the sclera. These cells maintain the physiological function, chemical composition, and biomechanical properties of the sclera via the secretion of collagen. Collagen I provides major structural support in the sclera, thereby maintaining its biomechanical integrity.[44] Scleral properties are influenced by three primary factors: the activity of scleral fibroblasts,[45] the structural characteristics of the sclera (including its thickness, stiffness, and collagen content),[9] and its hydration levels, which are regulated by glycosaminoglycans in the ECM.[9] Research has shown a close correlation between the elastic moduli of biological tissues and cells and their physiological activities and health status. If the sclera is modeled as a simple pressure vessel, its deformation during the development of myopia will be inversely proportional to its elastic modulus.[34] Multiple studies have demonstrated that imbalances in the upregulation and downregulation of MMP-2 lead to alterations in the biomechanical characteristics of the sclera,[46–48] and the content and arrangement of scleral collagen determine the biomechanical properties of the sclera.[25,44,49] In this study, we investigated the role of the Wnt7b/β-catenin signaling pathway in regulating the elastic modulus of the sclera during myopia progression. We found that FDM was linked to the activation of the Wnt7b/β-catenin signaling pathway, which promoted MMP-2 expression, reduced collagen I content, and decreased scleral stiffness. Scleral stiffness is primarily determined by its structure. The stiffness of the sclera is predominantly dictated by its collagen-dense extracellular matrix. During the development of myopia, collagen degradation results in scleral thinning, which not only compromises its structural integrity but also reduces it biomechanical resistance, leading to increases eye

Investigative Ophthalmology & Visual Science

elongation.[50] These scleral changes may lead to the establishment of a pathological feedback loop that accelerates myopia progression.

Limitations and Future Perspectives

On the basis of our findings, we propose that FDM activates the Wnt7b/β-catenin signaling pathway in the sclera. This activation upregulates the downstream target gene MMP-2, promoting collagen I degradation and progression of myopia. This process reduces the content of scleral collagen proteins and fibers, leading to decreased scleral stiffness, increased axial elongation, and further myopia progression. Although our study has provided valuable insights, it still has limitations. First, although we have demonstrated that the Wnt7b/β-catenin pathway regulates MMP-2–mediated collagen I degradation during the progression of myopia, further investigations are required to elucidate the direct role of this pathway in regulating collagen expression in normal eyes.[51–54] Second, the pharmacological inhibitors used in this study cannot completely block the effects of Wnt7b/β-catenin signaling and MMP-2 on downstream pathways. Conditional gene knockout models or gene-editing techniques would provide stronger evidence for our conclusions. Finally, the refraction and axial length were only measured at baseline and at 2 weeks after treatment, but additional measurements during the 2-week treatment period could potentially offer insights into the onset of the drug treatments.

Conclusions

In conclusion, our research confirmed that MMP-2 and the Wnt7b/β-catenin signaling pathway are crucial regulators of scleral ECM remodeling during myopia development. The activation of the Wnt7b/β-catenin pathway during myopia increases the expression of MMP-2, its downstream target gene, facilitating collagen I degradation. This process results in a decrease in the scleral collagen content and stiffness which in turn promotes axial ocular elongation and contributes to a myopic shift in refractive error. In addition to offering deeper insights into the mechanisms underlying myopia-related eye enlargement, our findings identified potential gene targets for further exploration in myopia treatment.

Acknowledgments

Supported by grants from the National Natural Science Foundation of China (82071002, 82271057, and 12372267), National Key R&D Program of China (2021YFA0719302), and Strategic Priority Research Program of the Chinese Academy of Sciences (XDB0620102).

The schematic illustrations in Figures 3b, 4a, and 6b were created with BioRender.com.

Disclosure: **B. Wen**, None; **H. Li**, None; **H. Tao**, None; **H. Ren**, None; **B. Ma**, None; **M. Shi**, None; **S. Chen**, None; **J. Du**, None; **Z. Cai**, None; **J. Zhang**, None; **D. Guan**; None; **Z. Deng**; None

References

1. Baird PN, Saw SM, Lanca C, et al. Myopia. *Nat Rev Dis Primer.* 2020;6(1):99.
2. Jost BJ, Marcus A, Pauline C, et al. IMI prevention of myopia and its progression. *Invest Ophthalmol Vis Sci.* 2021;62(5):6.
3. Ng DSC, Lai TYY. Insights into the global epidemic of high myopia and its implications. *JAMA Ophthalmol.* 2022;140(2):123–124.
4. Bourke CM, Loughman J, Flitcroft DI, Loskutova E, O'Brien C. We can't afford to turn a blind eye to myopia. *QJM.* 2023;116(8):635–639.
5. Arrigo A, Aragona E, Bianco L, et al. The clinical role of the choroidal assessment in high myopia: characteristics and association with neovascular and atrophic complications. *Invest Ophthalmol Vis Sci.* 2023;64(12):16.
6. Resnikoff S, Jonas JB, Friedman D, et al. Myopia – a 21st century public health issue. *Invest Ophthalmol Vis Sci.* 2019;60(3):Mi–Mii.
7. Ma YY, Wen YC, Zhong H, et al. Healthcare utilization and economic burden of myopia in urban China: a nationwide cost-of-illness study. *J Glob Health.* 2022;12:11003.
8. Jonas BJ, Jonas RA, Bikbov MM, Wang YX, Panda-Jonas S, Myopia: histology, clinical features, and potential implications for the etiology of axial elongation. *Prog Retin Eye Res.* 2023;96:101156.
9. McBrien NA, Gentle A. Role of the sclera in the development and pathological complications of myopia. *Prog Retin Eye Res.* 2003;22(3):307–338.
10. Yu Q, Zhou JB. Scleral remodeling in myopia development. *Int J Ophthalmol.* 2022;15(3):510–514.
11. Ikeda SI, Kurihara T, Toda M, Jiang X, Torii H, Tsubota K. Oral bovine milk lactoferrin administration suppressed myopia development through matrix metalloproteinase 2 in a mouse model. *Nutrients.* 2020;12(12):3744.
12. Lin MY, Lin IT, Wu YC, Wang IJ. Stepwise candidate drug screening for myopia control by using zebrafish, mouse, and Golden Syrian Hamster myopia models. *EBioMedicine.* 2021; 65:103263.
13. She M, Li T, Shi W, Li B, Zhou X. AREG is involved in scleral remodeling in form-deprivation myopia via the ERK1/2-MMP-2 pathway. *FASEB J.* 2022;36(5):e22289.
14. Lyu Y, Xiao Q, Yin L, Yang L, He W. Potent delivery of an MMP inhibitor to the tumor microenvironment with thermosensitive liposomes for the suppression of metastasis and angiogenesis. *Signal Transduct Target Ther.* 2019;4:26.
15. Zong L, Xu H, Zhang H, et al. A review of matrix metalloproteinase-2-sensitive nanoparticles as a novel drug delivery for tumor therapy. *Int J Biol Macromol.* 2024;262(Pt 2):130043.
16. Wu W, Su Y, Hu C, et al. Hypoxia-induced scleral HIF-2α upregulation contributes to rises in MMP-2 expression and myopia development in mice. *Invest Ophthalmol Vis Sci.* 2022;63(8):2.
17. Liu Z, Xiu Y, Qiu F, et al. Canonical Wnt signaling drives myopia development and can be pharmacologically modulated. *Invest Ophthalmol Vis Sci.* 2021;62(9):21.
18. Hu S, Ouyang S, Liu H, Zhang D, Deng Z. The effect of Wnt/β-catenin pathway on the scleral remodeling in the mouse during form deprivation. *Int Ophthalmol.* 2021;41(9):3099–107.
19. Miyake M, Yamashiro K, Tabara Y, et al. Identification of myopia-associated WNT7B polymorphisms provides insights into the mechanism underlying the development of myopia. *Nat Commun.* 2015;6:6689.
20. Li H, Lian X, Guan D. Crossover behavior in stress relaxations of poroelastic and viscoelastic dominant hydrogels. *Soft Matter.* 2023;19(29):5443–5451.
21. Moeendarbary E, Harris AR. Cell mechanics: principles, practices, and prospects. *Wiley Interdiscip Rev Syst Biol Med.* 2014;6(5):371–378.
22. Magazzù A, Marcuello C, Alessandro M, Carlos M. Investigation of soft matter nanomechanics by atomic force

Investigative Ophthalmology & Visual Science

microscopy and optical tweezers: a comprehensive review. *Nanomaterials (Basel)*. 2023;13(6):963.

23. Boote C, Sigal IA, Grytz R, Hua Y, Nguyen TD, Girard MJA. Scleral structure and biomechanics. *Prog Retin Eye Res*. 2020;74:100773.
24. Harper AR, Summers JA. The dynamic sclera: extracellular matrix remodeling in normal ocular growth and myopia development. *Exp Eye Res*. 2015;133:100–11.
25. Ouyang X, Han Y, Xie Y, et al. The collagen metabolism affects the scleral mechanical properties in the different processes of scleral remodeling. *Biomed Pharmacother*. 2019;118:109294.
26. Liu H, Chen D, Yang Z, Li X. Atropine affects the outer retina during inhibiting form deprivation myopia in guinea pigs. *Curr Eye Res*. 2022;47(4):614–623.
27. Schaeffel F, Hagel G, Eikermann J, Collett T. Lower-field myopia and astigmatism in amphibians and chickens. *J Opt Soc Am A Opt Image Sci Vis*. 1994;11(2):487–495.
28. Guan D, Shen Y, Zhang R, Huang P, Lai PY, Tong P. Unified description of compressive modulus revealing multiscale mechanics of living cells. *Phys Rev Res*. 2021;3(4):043166.
29. Tyagi SC, Ratajska A, Weber KT. Myocardial matrix metalloproteinase(s): localization and activation. *Mol Cell Biochem*. 1993;126(1):49–59.
30. Roczkowsky A, Chan BYH, Lee TYT, et al. Myocardial MMP-2 contributes to SERCA2a proteolysis during cardiac ischaemia–reperfusion injury. *Cardiovasc Res*. 2020;116(5):1021–1031.
31. Li Z, Cai X. Baicalein targets STMN1 to inhibit the progression of nasopharyngeal carcinoma via regulating the Wnt/β-catenin pathway. *Environ Toxicol*. 2024;39(5):3003–3013.
32. Deshmukh V, Murphy EA, Hood J, inventors. Methods of using indazole-3-carboxamides and their use as wnt/b-catenin signaling pathway inhibitors. US patent EP-3473099-A1. September 14, 2011.
33. Arensman MD, Kovochich AN, Kulikauskas RM, et al. WNT7B mediates autocrine Wnt/β-catenin signaling and anchorage-independent growth in pancreatic adenocarcinoma. *Oncogene*. 2014;33(7):899–908.
34. Xie Y, Ouyang X, Wang G. Mechanical strain affects collagen metabolism-related gene expression in scleral fibroblasts. *Biomed Pharmacother*. 2020;126:110095.
35. Zhao F, Wu H, Reinach PS, et al. Up-regulation of matrix metalloproteinase-2 by scleral monocyte-derived macrophages contributes to myopia development. *Am J Pathol*. 2020;190(9):1888–1908.
36. Lv X, Lai L, Xu Y, et al. Effects of riboflavin/ultraviolet-A scleral collagen cross-linking on regional scleral thickness and expression of MMP-2 and MT1-MMP in myopic guinea pigs. *PLoS One*. 2023;18(1):e0279111.
37. Suo NC, Lei CL, Zhang YC, Li CL, Li FZ, Gong K. Effects of latanoprost on the expression of TGF-β1 and Wnt /β-catenin signaling pathway in the choroid of form-deprivation myopia rats. *Cell Mol Biol (Noisy-le-grand)*. 2020;66(6):71–75.
38. Wen Y, Dai B, Zhang X, et al. Retinal transcriptomics analysis reveals the underlying mechanism of disturbed emmetropization induced by wavelength defocus. *Curr Eye Res*. 2022;47(6):908–917.
39. Lu SY, Tang SM, Li FF, et al. Association of *WNT7B* and *RSPO1* with axial length in school children. *Invest Ophthalmol Vis Sci*. 2020;61(10):11.
40. Liu J, Xiao Q, Xiao J, et al. Wnt/β-catenin signalling: function, biological mechanisms, and therapeutic opportunities. *Signal Transduct Target Ther*. 2022;7(1):3.
41. Chen Z, Xiao K, Long Q. Intraperitoneal injection of MCC950 inhibits the progression of myopia in form-deprivation myopic mice. *Int J Mol Sci*. 2023;24(21):15839.
42. Wang X, Lin Q, Liu S, et al. LncRNA-XR_002792574.1-mediated ceRNA network reveals potential biomarkers in myopia-induced retinal ganglion cell damage. *J Transl Med*. 2023;21(1):785.
43. Kang L, Ikeda S-I, Yang Y, et al. Establishment of a novel ER-stress induced myopia model in mice. *Eye Vis (Lond)*. 2023;10(1):44.
44. Wang C, Xie Y, Wang G. The elastic modulus and collagen of sclera increase during the early growth process. *J Mech Behav Biomed Mater*. 2018;77:566–571.
45. Lin X, Lei Y, Pan M, et al. Augmentation of scleral glycolysis promotes myopia through histone lactylation. *Cell Metab*. 2024;36(3):511–525.e7.
46. Gong B, Liu X, Zhang D, et al. Evaluation of MMP2 as a candidate gene for high myopia. *Mol Vis*. 2013;19:121–127.
47. Liu H-H, Kenning MS, Jobling AI, McBrien NA, Gentle A. Reduced scleral TIMP-2 expression is associated with myopia development: TIMP-2 supplementation stabilizes scleral biomarkers of myopia and limits myopia development. *Invest Ophthalmol Vis Sci*. 2017;58(4):1971–1981.
48. Chen B, Li X, Sun Y, et al. Study of the effects of rabbit scleral fibroblasts on cellular biomechanical properties and MMP-2 expression using two modes of riboflavin/ultraviolet A wave collagen cross-linking. *Exp Eye Res*. 2021;212:108695.
49. Sun X, Chen D, Liu X, Yan X, Wu Y. Effect of enzyme-induced collagen crosslinking on porcine sclera. *Biochem Biophys Res Commun*. 2020;528(1):134–139.
50. Sun Y, Sha Y, Yang J, et al. Collagen is crucial target protein for scleral remodeling and biomechanical change in myopia progression and control. *Heliyon*. 2024;10(15):e35313.
51. Wehner D, Tsarouchas TM, Michael A, et al. Wnt signaling controls pro-regenerative Collagen XII in functional spinal cord regeneration in zebrafish. *Nat Commun*. 2017;8(1):126.
52. Liu D, Du J, Xie H, et al. Wnt5a/β-catenin-mediated epithelial-mesenchymal transition: a key driver of subretinal fibrosis in neovascular age-related macular degeneration. *J Neuroinflammation*. 2024;21(1):75.
53. Roh MR, Kumar R, Rajadurai R, et al. Beta-catenin causes fibrotic changes in the extracellular matrix via upregulation of collagen I transcription. *Br J Dermatol*. 2017;177(1):312–315.
54. Kovács B, Vajda E, Nagy EE. Regulatory effects and interactions of the Wnt and OPG-RANKL-RANK signaling at the bone–cartilage interface in osteoarthritis. *Int J Mol Sci*. 2019;20(18):4653

Investigative Ophthalmology & Visual Science